Comparative sensitivity of proliferative and differentiated intestinal epithelial cells to the food contaminant, deoxynivalenol

Su Luo, Chloé Terciolo, Manon Neves, Sylvie Puel, Claire Naylies, Yannick Lippi, Philippe Pinton, Isabelle P. Oswald

Comparative sensitivity of proliferative and differentiated intestinal epithelial cells to the food contaminant, deoxynivalenol

Su Luo[1*], Chloe Terciolo[1*], Manon Neves[1], Sylvie Puel[1], Claire Naylies[1], Yannick Lippi[1], Philippe Pinton[1], Isabelle P. Oswald[1]

[1] Toxalim (Research Center in Food Toxicology), Université de Toulouse, INRAE, ENVT, INP-Purpan, UPS, Toulouse, France

*Both authors contributed equally to this manuscript

Corresponding author: Isabelle P. Oswald Isabelle.oswald@inrae.fr

Abstract: The intestinal epithelium is a functional and physical barrier formed by a cell monolayer that constantly differentiates from a stem cell in the crypt. This is the first target for food contaminants, especially mycotoxins. Deoxynivalenol (DON) is one of the most prevalent mycotoxins. This study compared the effects of DON (0-100µM) on proliferative and differentiated intestinal epithelial cells. Three cell viability assays (LDH release, ATP content and neutral red uptake) indicated that proliferative Caco-2 cells are more sensitive to DON than differentiated ones. The establishment of transepithelial electrical resistance (TEER), as a read out of the differentiation process, was delayed in proliferative cells after exposure to 1 µM DON. Transcriptome analysis of proliferative and differentiated exposure to 0-3 µM DON for 24 hours revealed 4,862 differentially expressed genes (DEG) and indicated an effect of both the differentiation status and the DON treatment. KEGG enrichment analysis indicated involvement of metabolism, ECM receptors and tight junctions in the differentiation process, while ribosome biogenesis, mRNA surveillance, and the MAPK pathway were involved in the response to DON. The number of differentially expressed genes and the amplitude of the effect were higher in proliferative cells exposed to DON than that in differentiated cells. In conclusion, our study shows that proliferative cells are more susceptible than differentiated ones to DON and that the mycotoxin delays the differentiation process.

Capsule: Proliferative intestinal epithelial cells are more susceptible than differentiated ones, to DON.

Key words: mycotoxin, cell toxicity, intestinal cell renewal, cell proliferation, cytotoxicity, intestinal barrier function

1. Introduction

Food safety is a major issue worldwide. The intestine is the first barrier against ingested toxicants, but also the first target organ for food contaminants. The intestinal epithelium provides a selective semi-permeable membrane that allows the absorption of nutrients, electrolytes and water while preventing the entrance of harmful substances (Pinton and Oswald, 2014; Terciolo et al., 2019). The epithelium undergoes rapid and continuous self-renewal and cell differentiation along the crypt-villus axis. The stem cells at the bottom of the crypts generate proliferative cells and deliver them to the top of villi. During their migration from the crypt to the villi, proliferative cells mainly differentiate to absorptive enterocytes (Clevers, 2013). The balance between proliferation and apoptosis of epithelial cells maintains the intestinal barrier function and gut homeostasis. Proliferative cells in the crypt differ structurally and functionally from differentiated enterocytes in the villi.

Mycotoxins are the most frequently occurring natural food contaminants in human food and animal feed. Among them, Deoxynivalenol (DON), a widespread trichothecene, is mainly produced by *Fusarium graminearum* and *F. culmorum*. It frequently contaminates cereals and cereal products. Indeed, DON was detected in almost half of 26,613 cereal samples collected from 21 European countries, with the highest levels observed in wheat, maize and oat grains (Knutsen et al., 2017). Several studies indicated that 40% to 98% of the adult population are exposed to this food contaminant (De Santis et al., 2019; Turner et al., 2008). Moreover, European surveys showed that the tolerable daily intake (TDI) of 1 µg/kg b.w./d established by EFSA is exceeded in parts of the population, especially in children (Knutsen et al., 2017; Vin et al., 2020).

At the molecular level, DON inhibits protein synthesis. It interacts with the peptidyl transferase region of the 60S ribosomal subunit, impairing the initiation and elongation of protein synthesis (Payros et al., 2016). This “ribotoxic stress” activates mitogen-activated protein kinases and their downstream pathways (Lucioli et al., 2013; Pestka, 2010). Acute exposure in human is associated with vomiting and bloody

diarrhea (Ruan et al., 2020). Chronic exposure to DON leads to reduced food consumption and reduced weight gain, neuro-endocrine changes as well as alteration of immune functions (Payros et al., 2016; Pestka, 2010; Robert et al., 2017).

DON also targets the intestine as described by our group and by others (Maresca, 2013; Pinton and Oswald, 2014). This mycotoxin alters the intestinal structure (García et al., 2018), impairs the expression of tight junction proteins (Pinton et al., 2012), and reduces the production of mucus (Pinton et al., 2015), leading to alteration of the barrier function (Pinton et al., 2009). DON also affects the formation of the brush border and expression of intestinal enzymes (Kasuga et al., 1998), reduces absorption of nutrients (Maresca et al., 2002), modulates intestinal microbiota (Payros et al., 2017; Waché et al., 2009), and increases the expression/secretion of pro-inflammatory cytokines in local immune responses (Payros et al., 2016; Pestka, 2010; Pinton and Oswald, 2014).

Despite this damage, the mechanisms underlying the effects of food contaminants on the proliferation and differentiation of intestinal cell have never been studied. The aim of this study was to better understand the impact of deoxynivalenol on intestinal disorders by analyzing its interaction with proliferative and differentiated cells in the gut. We studied the influence of DON on the differentiation process of the intestinal epithelium by measuring cytotoxicity and trans-epithelial electrical resistance (TEER), and by identifying the gene expression profile of proliferative and differentiated Caco-2 cells.

2. Materials and methods

2.1. Reagents

Purified DON (Sigma, St Quentin Fallavier, France) was dissolved in water stored at -20 °C. before being diluted in complete media DMEM-Glutamax medium (Life Technologies, Courtaboeuf, France) containing 5% fetal calf serum, 1% non-essential amino acid (Sigma) and 0.5% gentamycin (Eurobio, Courtaboeuf, France).

2.2. Cell culture

Caco-2 cells are able to undergo spontaneous and complete intestinal-like program differentiation (Hidalgo et al., 1989). They were cultured in complete medium, passaged by trypsinization at 80% confluence. Proliferative Caco-2 cells were analyzed at the sub-confluence stage; differentiated cells were allowed to differentiate for at least 14 days post-confluence.

2.3. Cytotoxicity assays

The cytotoxicity was measured by different indicators of cell viability or cell death: lactate dehydrogenase (LDH) release (Cytotox 96®, Promega, Charbonnières-les-Bains, France), amount of ATP (CellTiter-Glo®, Promega) and uptake of eurhodin dye (Neutral Red Cell Cytotoxicity, Clinisciences, Nanterre, France). Proliferative and differentiated cells were seeded in 96-well plates, grown for 24 hours or 21 days, exposed to DON (0-100 µM) for 48 hours then. Tests were performed according to the manufacturer's instructions.

2.4. Transepithelial electrical resistance (TEER) assay

Cells were seeded and cultured as previously described (Pinton et al., 2009), grown for 2 days or 14 days, then treated apically with DON. TEER was measured every 6 hours with a cellZscope (nanoAnalytics, Münster, Germany).

2.5 DNA labeling

At day 14 and 28, DNA labeling was performed on insert as surrogate marker of cell number. Cells were washed in PBS, directly fixed in the insert with 4%

paraformaldehyde in PBS (20 min, RT) and washed in PBS. Paraformaldehyde was neutralized with 20 mM NH_4Cl. Cells were washed in PBS, permeabilized with 0.2% Triton X-100 in PBS, washed in PST buffer (PBS, 2% fetal calf serum, 0.2% Triton X-100) and incubated with RedDot (Interchim, Montluçon, France) 1/500 dilution in PST. After 1 hour of incubation and washing in PST, DNA was quantified using an Odyssey Infrared Imaging Scanner (Li-Cor ScienceTec, Les Ulis, France) with the 680 nm fluorophore.

2.6 Microarray data processing and functional analysis of differentially expressed genes

Proliferative and differentiated cells were cultured in 6-well plates, grown for 2 or 21 days, and exposed to 3 µM DON for 24 hours. Total RNA was extracted as previously described (Alassane-Kpembi et al., 2017b); all the samples exhibited an RNA integrity number > 9.3.

Microarray experiments were conducted on the GeT-TriX platform using Agilent Sureprint G3 Human GE V3 microarrays (8 × 60K, design 072363) according to the manufacturer's instructions as already described (Alassane-Kpembi et al., 2017a). Hierarchical clustering analysis of probes was carried out on the MATRiX APP (http://matrix.toulouse.inra.fr/). Enrichment and functional analysis of DE genes in each cluster was analyzed using DAVID 6.8 (https://david.ncifcrf.gov/) and KOBAS 3.0 (http://kobas.cbi.pku.edu.cn/) with the database KEEG pathway and Gene Ontology. Only pathways with FDR p- value ≤ 0.05 were presented.

2.7 Quantitative real-time polymerase chain reaction (RT-qPCR)

Primers designed using PrimerQuest® software were purchased from Sigma (Table 1). RT-PCR assays were performed as previously described (Maruo et al., 2018). The expression values of the genes of interest were normalized against three housekeeping genes PSMB6, ACTB and GAPDH validated with NormFinder software. Gene expression is expressed relative to the control group.

2.8 Statistical analysis

Statistical analyses were performed using GraphPad Prism 4 (La Jolla, CA, USA). One-way ANOVA (non-parametric) or two-way ANOVA with a Bonferroni test were performed to analyze the differences between experimental groups. $p \leq 0.05$ was considered significant.

The R Bioconductor packages (www.bioconductor.org, v 3.6) and the limma lmFit function were used to analyze the microarray data as described previously (Alassane-Kpembi et al., 2017a). Probes with adjusted p-value (FDR correction using Benjamini-Hochberg method) ≤ 0.05 were considered to be differentially expressed between conditions. Hierarchical clustering was applied to the samples and probes using the 1-Pearson correlation coefficient as the distance and Ward's criterion for agglomeration. The results are presented as a heatmap of gene expression profiles.

3 Results

3.1 Determination of toxicity in proliferative and differentiated cells in response to DON

The comparative effect of DON on proliferative and differentiated cells was first assessed through cytotoxicity assays. Three different tests were used, one measuring LDH release, the second, ATP content, and the third, neural red uptake. As shown in figure 1A, DON at concentrations of up to 3 µM did not induce LDH release in either proliferative or differentiated cells. Concentrations of 10 and 30 µM DON caused the significant release of LDH in proliferative cells compared to untreated cells ($p < 0.001$). Similarly, concentrations of 30 and 100 µM DON caused the significant release of LDH in differentiated cells ($p < 0.001$). When exposed to 3 µM DON the LDH release in differentiated and proliferating cells were 99.7% and 181% of untreated control respectively. These values increased to 124% and 310% in differentiated and proliferating cells exposed to 10 µM DON and to 192% and 655% in cells exposed to 30 µM of toxins. To conclude, LDH release was significantly higher in proliferative cells exposed to DON than in differentiated cells ($p < 0.01$).

The cytotoxicity of DON was also analyzed using the CellTiter-Glo assay to quantify ATP content. Figure 1B shows that ATP content was not affected by DON at concentrations ranging from 0.01 to 0.3 µM in either proliferating or differentiated cells. By contrast, 1-30 µM DON markedly reduced ATP content in proliferative cells ($p < 0.001$). In differentiated cells, ATP content increased from 1 to 30 µM DON ($p < 0.001$). Only the highest concentration of DON (100 µM) reduced the ATP content ($p < 0.001$). The ATP content in proliferating and differentiated cells exposed to 10 µM DON were 55% and 134% of control; and 54% and 119% of control in proliferating and differentiated cells exposed to 30 µM DON. Thus, this cytotoxicity test also revealed higher sensitivity of proliferative Caco-2 to DON compared to that of differentiated cells.

The neutral red assay is based on selective uptake of eurhodin dye by viable cells and by the staining of their lysosomes. Eurhodin uptake was not affected by the concentrations of DON up to 0.3 µM in either proliferative or differentiated cells.

Conversely, uptake decreased significantly when proliferative and differentiated cells were exposed to 1- 30 µM DON and to 30 and 100 µM DON ($p < 0.001$), respectively. However, exposure to 1 to 100 µM DON led to a larger decrease in neutral red uptake in proliferative cells than in differentiated cells ($p < 0.001$) (figure 1C). The neutral red uptake were 95%, 93% and 85% of control in differentiated cells exposed to 3, 10 and 30 µM DON respectively; it decreased to 50%, 27% and 34% of control in proliferating cells exposed to the same concentrations of toxins.

Using three different tests, we thus demonstrated that the proliferative Caco-2 cells are more sensitive to DON toxicity than differentiated ones.

3.2 Effect of DON on the establishment and the persistence of the intestinal barrier integrity

Using the establishment of TEER as a readout, we next investigated the effect of DON on the differentiation processes. As shown in figure 2A, 10 days of culture were required for the monolayer to start differentiating and for the TEER to increase; the complete differentiation was assessed when the TEER reached a plateau after 16 days of cell culture. Exposure of undifferentiated cells to 0.3 µM DON had no effect on the differentiation process. Exposure to 1 µM slightly delayed the TEER at 16 days and exposure to 3 µM DON delayed the differentiation process between the 14th day and the 22nd day ($p < 0.001$). Nevertheless, after 24 days, the TEER of the monolayers exposed to 0.3 to 3 µM DON was the same as that of untreated cells. Conversely, the treatment of undifferentiated cells with 10 µM of DON did not allow the establishment of TEER. This relates to the toxicity of this concentration of DON observed on proliferation cells (figure 1). On the opposite, no effect on viability was observed on cells treated with 1 or 3 µM DON. Indeed, using DNA staining as a proxy of total cell number, we did not observed any changes throughout the experiment. At day 14, the DNA content of trans-well devices treated with 1 µM and 3 µM were 76 ± 7% and 96 ± 19% ($p>0.05$) of control wells respectively. At day 28, the values were 83 ± 8 % and 107 ± 26 % ($p>0.05$).

As shown in figure 2B, DON also modulated the TEER of differentiated cells. Indeed, exposure of differentiated cells to 0.3 and 1 µM of DON numerically decreased the TEER values but the effect was not statistically significant. By contrast, 3 and 10 µM of DON reduced the TEER by 22% ($p < 0.05$) and by 98% ($p < 0.001$), respectively. Of note, the decreased TEER observed at 10 µM on differentiated cells as early as 48 hours was not associated with an increased cytotoxicity of differentiated cell to the mycotoxin (figure 1).

Taken together, these data indicate that DON differentially influenced the intestinal barrier function during and after differentiation.

3.3 Comparative gene expression profiles of proliferative and differentiated intestinal epithelial cells in response to DON

To gain more insight into the comparative toxicity of DON for proliferative and differentiated intestinal cells, we used a genome wide transcriptomic approach. Microarray analysis identified 4,862 differentially expressed genes (DEG) with a fold change over 2 (FDR p-value ≤ 0.05, FC ≥ 2).

Principal component analysis (figure 3A) clearly separated four different groups and showed that cell status (proliferative versus differentiated) contributed up to 59% of the changes in gene expression, while DON treatment contributed 29%. The Venn diagram (figure 3B) highlights the cell status-dependent changes in gene expression upon exposure to DON. It shows that, among these DEG, 1,659 were specific to the proliferation status, 1,117 were specific to the differentiation status, and 1,043 genes overlap the two phenotypes. Figure 3B also shows that DON modulated 25% more genes in proliferative cells than in differentiated ones (2,702 versus 2,160 DE genes, respectively).

The 80 genes with the biggest changes caused by the DON treatment (down- and up-regulated) are shown in figure 3C. The figure also shows that DON had a similar effect on proliferative and differentiated cells but that the amplitude of the effect was higher in proliferative than in differentiated cells. These results were confirmed by

RT-qPCR for the representative up-regulated gene ANKRD1 and the representative down regulated gene MYBPH (figure 3D).

A supervised hierarchical clustering analysis was then performed using 5,843 probes representing 4,862 differentially expressed genes. The results are shown in figure 4. Four main clusters were identified; two clusters (clusters 1 and 3 containing 1,326 and 1,537 probes, respectively) illustrate a cell status effect; while a second set of clusters (clusters 2 and 4 containing 1,348 and 1,632 probes, respectively) illustrates the effect of exposure to DON. Clusters 1 and 3 comprise genes modulated by the differentiation process independently of DON exposure. Clusters 2 and 4 comprise genes whose expression is sensitive to DON whatever the phenotype of Caco-2 cells (figure 4).

Functional enrichment via KEGG and GO revealed that genes in cluster 1 are mainly involved in cell growth, including genes involved in the cell cycle in DNA replication, and in cellular senescence. Cluster 3 indicates that the main functions modulated by cell differentiation included genes involved in ECM-receptor interaction, tight junction and metabolism (figure 5). Functional enrichment analysis revealed that cluster 2 is composed of genes involved in several functions including ribosome biogenesis, mRNA surveillance, and the MAPK signaling pathway (figure 5), all linked with the ribotoxic stress. Analysis of cluster 4 revealed that the main pathways down-regulated upon DON exposure are differentiation processes and intestinal functions such as cholesterol metabolism, metabolic pathway, and protein digestion and absorption. We examined 18 genes (8 regulated by cell status and 10 regulated by DON) using qRT-PCR to confirm the changes observed in the microarray (figure 6). For cluster 1, we chose genes involved in the progression of the cell cycle through mitotic events to confirm the effect of differentiation. *PLK1* is a serine/threonine-protein kinase involved in functional maturation of the centrosome in late G2 and in the establishment of the bipolar spindle, whereas *CDC20* (cell-division cycle) activates the anaphase promoting complex (APC/C) that initiates chromatid separation and entrance into anaphase. The serine/threonine kinase *BUB1* plays the role of mitotic checkpoint and cyclinA2 (*CCNA2*) is tightly linked to the progression

of the cell cycle. All these characteristic genes in cluster 1 (*PLK1, BUB1, CDC20*, *CCNA2* genes) were down-regulated in differentiated cells.

Selected genes from cluster 3 (such as *CRYL, CEL, NPNT* and *LAMC2* genes) are involved in cell adhesion and metabolic pathways. The Laminin Subunit Gamma 2 *(LAMC2*) is a major constituent of basement membrane, and is involved in cell adhesion, migration, and differentiation processes as well as nephronectin (*NPNT*), ligand belonging to the family of integrins involved in development, differentiation, and adhesion processes. Genes involved in the digestion and absorption of lipid nutrients were also selected: Lambda-crystallin 1 (*CRYL1)* and carboxyl ester lipase (*CEL*). All these genes were up-regulated in differentiated cells.

Characteristic genes were selected in cluster 2 (ribosomal RNA small subunit methyltransferase NEP1 (*EMG1*), NIN1 Binding Protein 1 Homolog (*NOB1*) and Serine/threonine-protein kinase (*RIOK2*)) are involved in the maturation of ribosomal subunits (40s and 60s), in ribosome assembly in nucleolus and protein synthesis (RNA-binding protein 28, *RBM28* and RNA Polymerase II subunit A, *POLR2A*). The expression of representative genes in cluster 2 (*EMG1, NOB1, RIOK2, RBM28, POLR2A*), confirmed up-regulation of gene expression in response to DON.

Genes in cluster 4 are more involved in cell functions; Lipase A (*LIPA*), responsible for cholesterol degradation for use by the cell; *KCNN4 (*heterotetrameric voltage-independent potassium channel*)* which leads to membrane hyperpolarization after its activation and promotes calcium influx, whereas *XPNPEP2* (X-Propyl Aminopeptidase P), involved in collagen, peptide and cytokine degradation, was down-regulated upon DON exposure.

4 Discussion

The barrier function of the intestinal epithelium is regulated by the villus and crypt compartments together. Proliferative cells in the crypt are structurally and functionally different from the differentiated enterocytes in the villi (Beaulieu, 1999; Gordon and Hermiston, 1994; Montgomery et al., 1999; Tan and Barker, 2014). Although the adverse effects of mycotoxins, especially those of DON, on the intestinal functions are well described (Payros et al., 2016; Pinton et al., 2015, 2012) the comparative effect of DON, and more generally of any toxic compound, on villus and crypt cells is largely unknown. The aim of this study was thus to describe the effects of DON on proliferative and differentiated intestinal cells by measuring cytotoxicity, trans-epithelial electrical resistance (TEER), and gene expression profiles. This comparison was performed on the human Caco-2 enterocyte-like model, as these cells spontaneously differentiate to polarized monolayer with the morphological and biochemical properties of small intestinal enterocytes (Luo et al., 2019; Pinton et al., 2009; Sambruy et al., 2001).

In the present study, we observed that DON caused higher toxicity in proliferating cells than in differentiated ones. We also observed that DON at concentration of 1 µM and above delayed the differentiation process. In line with our results, Wang and al., showed that DON at 5 µM reduced protein expression of claudin-3, 4 and occludin in proliferative cells, whereas it only reduced protein expression in claudin-4 in differentiated cells (Wang et al., 2019). Two other studies reported similar toxicity of zinc in Caco-2 cells whatever their differentiation status (Scarino et al., 1992; Zödl et al., 2003).

We compared the cytotoxicity of DON for proliferative and differentiated Caco-2 cells using three different methods, LDH release, ATP content and neutral red uptake. Whatever the test, proliferative cells were found to be more sensitive to DON than differentiated cells. The high sensitivity of proliferative cells to DON has already been reported in Caco-2 cells as well as in the IPEC-J2 porcine intestinal epithelial cell line (Awad et al., 2012; Pierron et al., 2016; Ying et al., 2019). The greater

sensitivity of proliferative cells could be due to the primary feature of DON toxicity. Indeed, the ribotoxic stress response-mediated inhibition of protein synthesis (Pan et al., 2014; Zhou et al., 2014), is more important for dividing cells than for differentiated cells as proliferating cells need a large amount of RNA, DNA and protein synthesis (Fortin-Magana et al., 1970, Pestka et al 2010).

Perturbation of proliferation affects cell migration along the villus. Indeed, using cell-labelling, Parker et al. (2017) demonstrated a relation between cell proliferation rates and epithelial cell migration velocities and concluded that cell proliferation within the crypt is the primary force driving cell migration along the villus. These toxic effects may cause morphological alterations of the intestinal tissue. Alterations in villus architecture (increased villus fusion and shorter villi) associated with necrosis and edema have already been observed both in intestinal explants (Pinton et al., 2012) and *in vivo* (Luo et al., 2019).

Measurement of TEER was used to assess the effect of DON on the differentiation process as well as on the establishment of mature and functional monolayer. In differentiated Caco-2 cells, TEER values were significantly reduced after 20 days exposure to 3 and 10 µM DON, as previously described in several intestinal cell lines (Luo et al., 2019; Maresca et al., 2002; Pinton et al., 2009). This reduced intestinal barrier function was associated with the disruption of tight junctions, mediated by activation of DON-induced MAPKs (Pinton et al., 2010; Springler et al., 2016). Increased intestinal permeability exposes the sub-epithelial tissues to luminal pathogens including bacterial translocation and can trigger inappropriate immune and inflammatory responses (Alassane-Kpembi et al., 2017b; Cano et al., 2013). In the proliferative cells, low doses of DON (1–3 µM) delayed the establishment of the TEER. We hypothesize that this will reduce the renewal and repair of the epithelium and reduce intestinal absorption and the barrier function (Piche, 2014; Wu et al., 2014). It is noteworthy that these effects can be linked to the growth deficiency and anorexia observed in presence of DON (Terciolo et al., 2018; Yunus et al., 2012) but also to the susceptibility of the host to develop bacterial infections and intestinal chronic disorders (Maresca, 2013; Payros et al., 2020).

A transcriptome analysis was performed to further delineate the toxicity of DON in differentiated and proliferative cells. We observed that DON modulates the expression of a larger number of genes (25% increase) in proliferative cells than in differentiated intestinal cells. The amplitude of the effect was also higher in proliferative than in differentiated cells.

In response to DON exposure, genes involved in ribosome biogenesis, mRNA surveillance, and in the MAPK signaling pathway were up-regulated in both proliferative and differentiated Caco-2 cells. Indeed, DON-induced ribotoxic stress impacts the regulation of the transcription as well as epigenetic factors, which may affect all the processes of RNA maturation and translation (mRNA surveillance, ribosome biogenesis, and mRNA transport). Among the genes involved in these signaling pathways, ribosome biogenesis is a fine-tuning of translation that likely occurs early before the onset of translation inhibition (Pan et al., 2013). We observed that DON increased gene expression of RNA biosynthesis (*EMG1*), RNA processing, and RNA maturation (*NOB1*, *WDR33, RIOK2*) as well as of Eukaryotic Initiation Factors (eIFs) kinases that control the translation initiation process (Roux and Topisirovic, 2018). DON controls gene expression by activating PKR that inhibits global translation but induces specific translation of pro-inflammatory genes by phosphorylating eIF2α (Piazzi et al., 2019). Modulation of transcriptional activity is a hallmark of cell response to stress. Integrated stress response leads to the restoration of cellular homeostasis to compensate for excessive apoptosis and for the reduced proliferation rate observed in intestinal epithelia cells, which, in turn, leads to a delay in TEER establishment. If this stress cannot be resolved and general translation remains inhibited, the cell will likely die due to the apoptosis mechanism (Piazzi et al., 2019). In addition, increased expression of some genes involved in mRNA transport (*PRMT5*) was observed after DON exposure. PRMT5-regulated processes caused MAPk activation. An increase in the number of genes involved in these pathways was associated with increased cytotoxicity in proliferative cells. What is more, ribotoxic stress induced by DON binding to ribosomes can rapidly activate the MAPK signaling

pathway leading to inflammation or ribosome RNA cleavage and hence, to cell apoptosis (He et al., 2012; Pestka, 2008).

Genes involved in cholesterol metabolism, protein digestion and absorption, and in metabolic pathways were down-regulated upon DON exposure. Cholesterol is a key component of cell membrane and is therefore necessary for cell growth, proliferation and differentiation, and excessive synthesis of cholesterol induced differentiation defects has been reported (Stange et al., 1988; Suzuki et al., 2019). In the present study, the DON-suppression of genes involved in cholesterol efflux such as *LIPA* and *CYP27A1* might lead to accumulation of cholesterol in cells, thereby inhibiting cell differentiation.

5 Conclusion

Our study highlights the fact that the state of differentiation of the cell layer is an important determinant of the response to exogenous substances and food contaminants. DON affects not only the ability of Caco-2 cells to proliferate but also their ability to form an impermeable barrier to protect the underlying tissue. Defective epithelial differentiation and altered function of the mucosal barrier may lead to the translocation of luminal bacteria within the body and potentially to chronic disorders such as inflammatory bowel disease. Disturbance of these processes can result in chronic inflammation and in anorexigenic effects of DON (Payros et al., 2020; Pinton and Oswald, 2014).

Acknowledgements: We are grateful to Ms Goodfellow for the English correction. This work was supported, in part, by the Genofood ANR project (19-CE34). Su Luo was supported by the China Scholarship Council.

3. References

Alassane-Kpembi, I., Gerez, J.R., Cossalter, A.-M., Neves, M., Laffitte, J., Naylies, C., Lippi, Y., Kolf-Clauw, M., Bracarense, A.P.L., Pinton, P., Oswald, I.P., 2017a. Intestinal toxicity of the type B trichothecene mycotoxin fusarenon-X: whole transcriptome profiling reveals new signaling pathways. Sci. Rep. 7, 7530. https://doi.org/10.1038/s41598-017-07155-2

Alassane-Kpembi, I., Puel, O., Pinton, P., Cossalter, A.-M., Chou, T.-C., Oswald, I.P., 2017b. Co-exposure to low doses of the food contaminants deoxynivalenol and nivalenol has a synergistic inflammatory effect on intestinal explants. Arch. Toxicol. 91, 2677–2687. https://doi.org/10.1007/s00204-016-1902-9

Awad, W.A., Aschenbach, J.R., Zentek, J., 2012. Cytotoxicity and metabolic stress induced by deoxynivalenol in the porcine intestinal IPEC-J2 cell line. J. Anim. Physiol. Anim. Nutr. 96, 709–716. https://doi.org/10.1111/j.1439-0396.2011.01199.x

Beaulieu, J.F., 1999. Integrins and human intestinal cell functions. Front. Biosci. 4, D310-321. https://doi.org/10.2741/beaulieu

Cano, P.M., Seeboth, J., Meurens, F., Cognie, J., Abrami, R., Oswald, I.P., Guzylack-Piriou, L., 2013. Deoxynivalenol as a new factor in the persistence of intestinal inflammatory diseases: an emerging hypothesis through possible modulation of Th17-mediated response. PLoS ONE 8, e53647. https://doi.org/10.1371/journal.pone.0053647

Clevers, H., 2013. The intestinal crypt, a prototype stem cell compartment. Cell 154, 274–284. https://doi.org/10.1016/j.cell.2013.07.004

De Santis, B., Debegnach, F., Miano, B., Moretti, G., Sonego, E., Chiaretti, A., Buonsenso, D., Brera, C., 2019. Determination of Deoxynivalenol Biomarkers in Italian Urine Samples. Toxins 11, 441. https://doi.org/10.3390/toxins11080441

Fortin-Magana, R., Hurwitz, R., Herbst, J.J., Kretchmer, N., 1970. Intestinal Enzymes: Indicators of Proliferation and Differentiation in the Jejunum. Science 167, 1627–1628. https://doi.org/10.1126/science.167.3925.1627

García, G.R., Payros, D., Pinton, P., Dogi, C.A., Laffitte, J., Neves, M., González Pereyra, M.L., Cavaglieri, L.R., Oswald, I.P., 2018. Intestinal toxicity of deoxynivalenol is limited by Lactobacillus rhamnosus RC007 in pig jejunum explants. Arch. Toxicol. 92, 983–993. https://doi.org/10.1007/s00204-017-2083-x

Gordon, J.I., Hermiston, M.L., 1994. Differentiation and self-renewal in the mouse gastrointestinal epithelium. Curr. Opin. Cell Biol. 6, 795–803. https://doi.org/10.1016/0955-0674(94)90047-7

He, K., Zhou, H.-R., Pestka, J.J., 2012. Targets and intracellular signaling mechanisms for deoxynivalenol-induced ribosomal RNA cleavage. Toxicol. Sci. 127, 382–390. https://doi.org/10.1093/toxsci/kfs134

Hidalgo, I.J., Raub, T.J., Borchardt, R.T., 1989. Characterization of the Human Colon Carcinoma Cell Line (Caco-2) as a Model System for Intestinal Epithelial Permeability. Gastroenterology 96, 736–749. https://doi.org/10.1016/S0016-5085(89)80072-1

Kasuga, F., Hara-Kudo, Y., Saito, N., Kumagai, S., Sugita-Konishi, Y., 1998. In Vitro Effect of Deoxynivalenol on the Differentiation of Human Colonic Cell Lines Caco-2 and t84. Mycopathologia 142, 161–167. https://doi.org/10.1023/A:1006923808748

Knutsen, H.K., Alexander, J., Barregård, L., Bignami, M., Brüschweiler, B., Ceccatelli, S., Cottrill, B., Dinovi, M., Grasl-Kraupp, B., Hogstrand, C., Hoogenboom, L. (Ron), Nebbia, C.S., Oswald, I.P., Petersen, A., Rose, M., Roudot, A.-C., Schwerdtle, T., Vleminckx, C., Vollmer, G., Wallace, H., Saeger, S.D., Eriksen, G.S., Farmer, P., Fremy, J.-M., Gong, Y.Y., Meyer, K., Naegeli, H., Parent-Massin, D., Rietjens, I., Egmond, H. van, Altieri, A., Eskola, M., Gergelova, P., Bordajandi, L.R., Benkova, B., Dörr, B., Gkrillas, A., Gustavsson, N., Manen, M. van, Edler, L., 2017. Risks to human and

animal health related to the presence of deoxynivalenol and its acetylated and modified forms in food and feed. EFSA J. 15, e04718. https://doi.org/10.2903/j.efsa.2017.4718

Lucioli, J., Pinton, P., Callu, P., Laffitte, J., Grosjean, F., Kolf-Clauw, M., Oswald, I.P., Bracarense, A.P.F.R.L., 2013. The food contaminant deoxynivalenol activates the mitogen activated protein kinases in the intestine: interest of ex vivo models as an alternative to in vivo experiments. Toxicon 66, 31–36. https://doi.org/10.1016/j.toxicon.2013.01.024

Luo, S., Terciolo, C., Bracarense, A.P.F.L., Payros, D., Pinton, P., Oswald, I.P., 2019. In vitro and in vivo effects of a mycotoxin, deoxynivalenol, and a trace metal, cadmium, alone or in a mixture on the intestinal barrier. Environ. Int. 132, 105082. https://doi.org/10.1016/j.envint.2019.105082

Maresca, M., 2013. From the gut to the brain: journey and pathophysiological effects of the food-associated trichothecene mycotoxin deoxynivalenol. Toxins 5, 784–820. https://doi.org/10.3390/toxins5040784

Maresca, M., Mahfoud, R., Garmy, N., Fantini, J., 2002. The mycotoxin deoxynivalenol affects nutrient absorption in human intestinal epithelial cells. J. Nutr. 132, 2723–2731. https://doi.org/10.1093/jn/132.9.2723

Maruo, V.M., Bracarense, A.P., Metayer, J.-P., Vilarino, M., Oswald, I.P., Pinton, P., 2018. Ergot Alkaloids at Doses Close to EU Regulatory Limits Induce Alterations of the Liver and Intestine. Toxins 10, 183. https://doi.org/10.3390/toxins10050183

Montgomery, R.K., Mulberg, A.E., Grand, R.J., 1999. Development of the human gastrointestinal tract: Twenty years of progress. Gastroenterology 116, 702–731. https://doi.org/10.1016/S0016-5085(99)70193-9

Pan, X., Whitten, D.A., Wilkerson, C.G., Pestka, J.J., 2014. Dynamic Changes in Ribosome-Associated Proteome and Phosphoproteome During Deoxynivalenol-Induced Translation Inhibition and Ribotoxic Stress. Toxicol. Sci. 138, 217–233. https://doi.org/10.1093/toxsci/kft270

Pan, X., Whitten, D.A., Wu, M., Chan, C., Wilkerson, C.G., Pestka, J.J., 2013. Global Protein Phosphorylation Dynamics during Deoxynivalenol-Induced Ribotoxic Stress Response in the Macrophage. Toxicol. Appl. Pharmacol. 268, 201–211. https://doi.org/10.1016/j.taap.2013.01.007

Payros, D., Alassane-Kpembi, I., Pierron, A., Loiseau, N., Pinton, P., Oswald, I.P., 2016. Toxicology of deoxynivalenol and its acetylated and modified forms. Arch. Toxicol. 90, 2931–2957. https://doi.org/10.1007/s00204-016-1826-4

Payros, D., Dobrindt, U., Martin, P., Secher, T., Bracarense, A.P.F.L., Boury, M., Laffitte, J., Pinton, P., Oswald, E., Oswald, I.P., 2017. The Food Contaminant Deoxynivalenol Exacerbates the Genotoxicity of Gut Microbiota. mBio 8. https://doi.org/10.1128/mBio.00007-17

Payros, D., Ménard, S., Laffitte, J., Neves, M., Tremblay-Franco, M., Luo, S., Fouche, E., Snini, S.P., Theodorou, V., Pinton, P., Oswald, I.P., 2020. The food contaminant, deoxynivalenol, modulates the Thelper/Treg balance and increases inflammatory bowel diseases. Arch. Toxicol. 94, 3173-3184; https://doi.org/10.1007/s00204-020-02817-z

Pestka, J.J., 2010. Deoxynivalenol: mechanisms of action, human exposure, and toxicological relevance. Arch. Toxicol. 84, 663–679. https://doi.org/10.1007/s00204-010-0579-8

Pestka, J.J., 2008. Mechanisms of deoxynivalenol-induced gene expression and apoptosis. Food Addit Contam Part A Chem Anal Control Expo Risk Assess 25, 1128–1140. https://doi.org/10.1080/02652030802056626

Piazzi, M., Bavelloni, A., Gallo, A., Faenza, I., Blalock, W.L., 2019. Signal Transduction in Ribosome Biogenesis: A Recipe to Avoid Disaster. Int. J. Mol. Sci. 20, 2718. https://doi.org/10.3390/ijms20112718

Piche, T., 2014. Tight junctions and IBS - the link between epithelial permeability, low-grade inflammation, and symptom generation? Neurogastroenterol. Motil. 26, 296–302. https://doi.org/10.1111/nmo.12315

Pierron, A., Mimoun, S., Murate, L.S., Loiseau, N., Lippi, Y., Bracarense, A.-P.F.L., Liaubet, L., Schatzmayr, G., Berthiller, F., Moll, W.-D., Oswald, I.P., 2016.

Intestinal toxicity of the masked mycotoxin deoxynivalenol-3-β-D-glucoside. Arch. Toxicol. 90, 2037–2046. https://doi.org/10.1007/s00204-015-1592-8

Pinton, P., Braicu, C., Nougayrede, J.-P., Laffitte, J., Taranu, I., Oswald, I.P., 2010. Deoxynivalenol impairs porcine intestinal barrier function and decreases the protein expression of claudin-4 through a mitogen-activated protein kinase-dependent mechanism. J. Nutr. 140, 1956–1962. https://doi.org/10.3945/jn.110.123919

Pinton, P., Graziani, F., Pujol, A., Nicoletti, C., Paris, O., Ernouf, P., Di Pasquale, E., Perrier, J., Oswald, I.P., Maresca, M., 2015. Deoxynivalenol inhibits the expression by goblet cells of intestinal mucins through a PKR and MAP kinase dependent repression of the resistin-like molecule β. Mol Nutr Food Res 59, 1076–1087. https://doi.org/10.1002/mnfr.201500005

Pinton, P., Nougayrède, J.-P., Del Rio, J.-C., Moreno, C., Marin, D.E., Ferrier, L., Bracarense, A.-P., Kolf-Clauw, M., Oswald, I.P., 2009. The food contaminant deoxynivalenol, decreases intestinal barrier permeability and reduces claudin expression. Toxicol. Appl. Pharmacol. 237, 41–48. https://doi.org/10.1016/j.taap.2009.03.003

Pinton, P., Oswald, I.P., 2014. Effect of deoxynivalenol and other Type B trichothecenes on the intestine: a review. Toxins 6, 1615–1643. https://doi.org/10.3390/toxins6051615

Pinton, P., Tsybulskyy, D., Lucioli, J., Laffitte, J., Callu, P., Lyazhri, F., Grosjean, F., Bracarense, A.P., Kolf-Clauw, M., Oswald, I.P., 2012. Toxicity of deoxynivalenol and its acetylated derivatives on the intestine: differential effects on morphology, barrier function, tight junction proteins, and mitogen-activated protein kinases. Toxicol. Sci. 130, 180–190. https://doi.org/10.1093/toxsci/kfs239

Robert, H., Payros, D., Pinton, P., Théodorou, V., Mercier-Bonin, M., Oswald, I.P., 2017. Impact of mycotoxins on the intestine: are mucus and microbiota new targets? J. Toxicol. Environ. Health, B Crit. Rev. 20, 249–275. https://doi.org/10.1080/10937404.2017.1326071

Roux, P.P., Topisirovic, I., 2018. Signaling Pathways Involved in the Regulation of mRNA Translation. Mol. Cell. Biol. 38, e00070-18. https://doi.org/10.1128/MCB.00070-18

Ruan, F., Chen, J.G., Chen, L., Lin, X. tian, Zhou, Y., Zhu, K. jing, Guo, Y.T., Tan, A.J., 2020. Food Poisoning Caused by Deoxynivalenol at a School in Zhuhai, Guangdong, China, in 2019. Foodborne Pathog. Dis. 17, 429-433. https://doi.org/10.1089/fpd.2019.2710

Sambruy, Y., Ferruzza, S., Ranaldi, G., De Angelis, I., 2001. Intestinal cell culture models: applications in toxicology and pharmacology. Cell Biol. Toxicol. 17, 301–317. https://doi.org/10.1023/A:1012533316609

Scarino, M.L., Poverini, R., Di Lullo, G., Bises, G., 1992. Inhibition of protein synthesis after exposure of Caco2 cells to heavy metals. Alternatives to laboratory animals: ATLA-Altern. Lab. Anim. 20, 325-333.

Springler, A., Hessenberger, S., Schatzmayr, G., Mayer, E., 2016. Early Activation of MAPK p44/42 Is Partially Involved in DON-Induced Disruption of the Intestinal Barrier Function and Tight Junction Network. Toxins 8. https://doi.org/10.3390/toxins8090264

Stange, E.F., Preclik, G., Schneider, A., Reimann, F., 1988. The role of enterocyte cholesterol metabolism in intestinal cell growth and differentiation. Scand. J. Gastroenterol. Suppl. 151, 79-85. https://doi.org/10.3109/00365528809095917

Suzuki, A., Shim, J., Ogata, K., Yoshioka, H., Iwata, J., 2019. Cholesterol metabolism plays a crucial role in the regulation of autophagy for cell differentiation of granular convoluted tubules in male mouse submandibular glands. Development 146. https://doi.org/10.1242/dev.178335

Tan, D.W.-M., Barker, N., 2014. Chapter Three - Intestinal Stem Cells and Their Defining Niche, in: Rendl, M. (Ed.), Current Topics in Developmental Biology, Stem Cells in Development and Disease. Academic Press, pp. 77–107. https://doi.org/10.1016/B978-0-12-416022-4.00003-2

Terciolo, C., Dapoigny, M., Andre, F., 2019. Beneficial effects of Saccharomyces boulardii CNCM I-745 on clinical disorders associated with intestinal barrier

disruption. Clin Exp Gastroenterol 12, 67–82. https://doi.org/10.2147/CEG.S181590

Terciolo, C., Maresca, M., Pinton, P., Oswald, I.P., 2018. Review article: Role of satiety hormones in anorexia induction by Trichothecene mycotoxins. Food Chem. Toxicol. 121, 701–714. https://doi.org/10.1016/j.fct.2018.09.034

Turner, P.C., Rothwell Joseph A., White Kay L.M., Gong YunYun, Cade Janet E., Wild Christopher P., 2008. Urinary Deoxynivalenol Is Correlated with Cereal Intake in Individuals from the United Kingdom. Environ. Health Perspect. 116, 21–25. https://doi.org/10.1289/ehp.10663

Vin, K., Rivière, G., Leconte, S., Cravedi, J.-P., Fremy, J.M., Oswald, I.P., Roudot, A.-C., Vasseur, P., Jean, J., Hulin, M., Sirot, V., 2020. Dietary exposure to mycotoxins in the French infant total diet study. Food Chem. Toxicol. 140, 111301. https://doi.org/10.1016/j.fct.2020.111301

Waché, Y.J., Valat, C., Postollec, G., Bougeard, S., Burel, C., Oswald, I.P., Fravalo, P., 2009. Impact of deoxynivalenol on the intestinal microflora of pigs. Int. J. Mol. Sci. 10, 1–17. https://doi.org/10.3390/ijms10010001

Wang, X., Li, L., Zhang, G., 2019. Impact of deoxynivalenol and kaempferol on expression of tight junction proteins at different stages of Caco-2 cell proliferation and differentiation. RSC Adv. 9, 34607–34616. https://doi.org/10.1039/C9RA06222J

Wu, M., Xiao, H., Ren, W., Yin, J., Tan, B., Liu, G., Li, L., Nyachoti, C.M., Xiong, X., Wu, G., 2014. Therapeutic Effects of Glutamic Acid in Piglets Challenged with Deoxynivalenol. PLOS ONE 9, e100591. https://doi.org/10.1371/journal.pone.0100591

Ying, C., Hong, W., Nianhui, Z., Chunlei, W., Kehe, H., Cuiling, P., 2019. Nontoxic concentrations of OTA aggravate DON-induced intestinal barrier dysfunction in IPEC-J2 cells via activation of NF-κB signaling pathway. Toxicol. Lett. 311, 114–124. https://doi.org/10.1016/j.toxlet.2019.04.021

Yunus, A.W., Blajet-Kosicka, A., Kosicki, R., Khan, M.Z., Rehman, H., Böhm, J., 2012. Deoxynivalenol as a contaminant of broiler feed: intestinal development,

absorptive functionality, and metabolism of the mycotoxin. Poult. Sci. 91, 852–861. https://doi.org/10.3382/ps.2011-01903

Zhou, H.-R., He, K., Landgraf, J., Pan, X., Pestka, J.J., 2014. Direct activation of ribosome-associated double-stranded RNA-dependent protein kinase (PKR) by deoxynivalenol, anisomycin and ricin: a new model for ribotoxic stress response induction. Toxins 6, 3406–3425. https://doi.org/10.3390/toxins 6123 406

Zödl, B., Zeiner, M., Sargazi, M., Roberts, N.B., Marktl, W., Steffan, I., Ekmekcioglu, C., 2003. Toxic and biochemical effects of zinc in Caco-2 cells. J. Inorg. Biochem. 97, 324–330. https://doi.org/10.1016/s0162-0134(03)00312-x

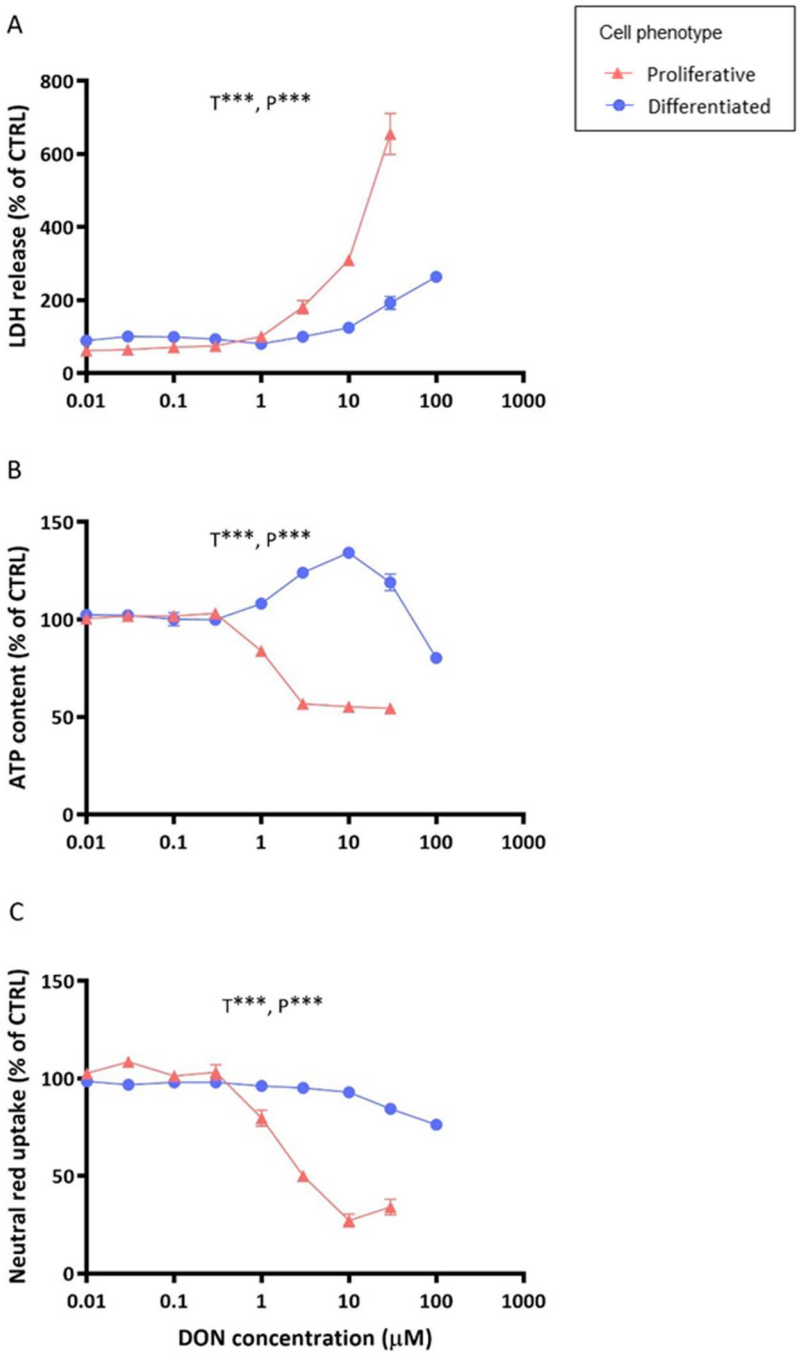

1

2 Figure 1. Cytotoxicity of DON on proliferative and differentiated Caco-2 cells

3 Cells were seeded in 96-well plates and cultured for 2 d (proliferative cells) or 21 d
4 (differentiated cells) before DON treatment. After 48h, LDH release (A), ATP content
5 (B) and neutral red uptake (C) were measured. Values are expressed as percent of
6 untreated cells. Results are expressed as the mean of 3 independent experiments ±
7 SEM. Data were analyzed by two-way ANOVA with Bonferroni post-test, T:
8 treatment effect; P: phenotype effect, *$p < 0.05$; **$p < 0.01$; ***$p < 0.001$.

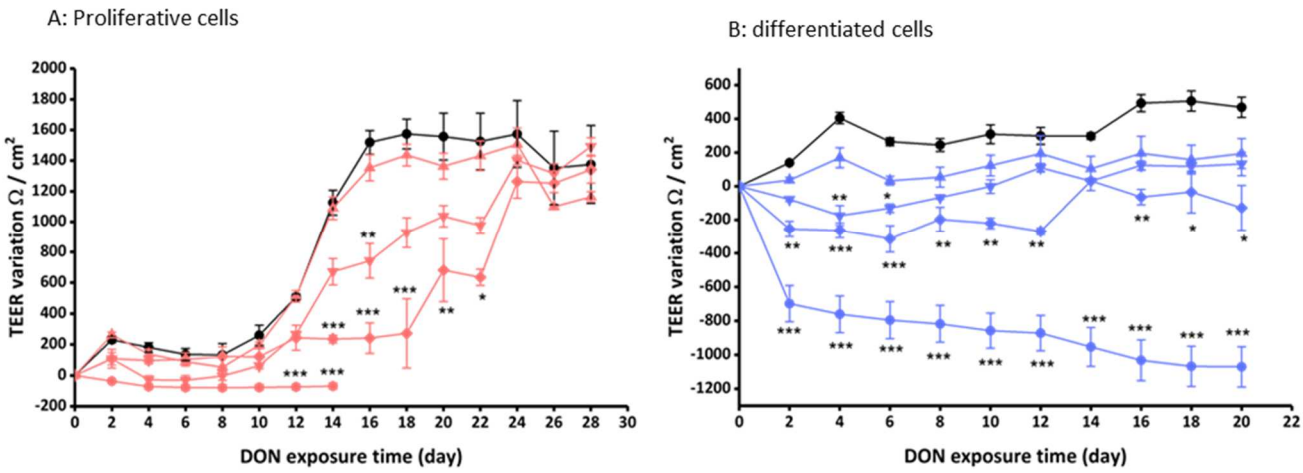

Figure 2. Effects of DON on the establishment and maintenance of TEER in Caco-2 cells.

Proliferative (A) or differentiated (B) Caco-2 cells cultivated on insert were treated apically with 0 (●), 0.3 (▲), 1 (▼), 3 (♦) and 10 (●) µM DON, and the TEER measured. Results are expressed as TEER variation after DON addition, mean of 3 independent experiments ± SEM. Data were analyzed by non-parametric one-way ANOVA; *$p < 0.05$; **$p < 0.01$; ***$p < 0.001$.

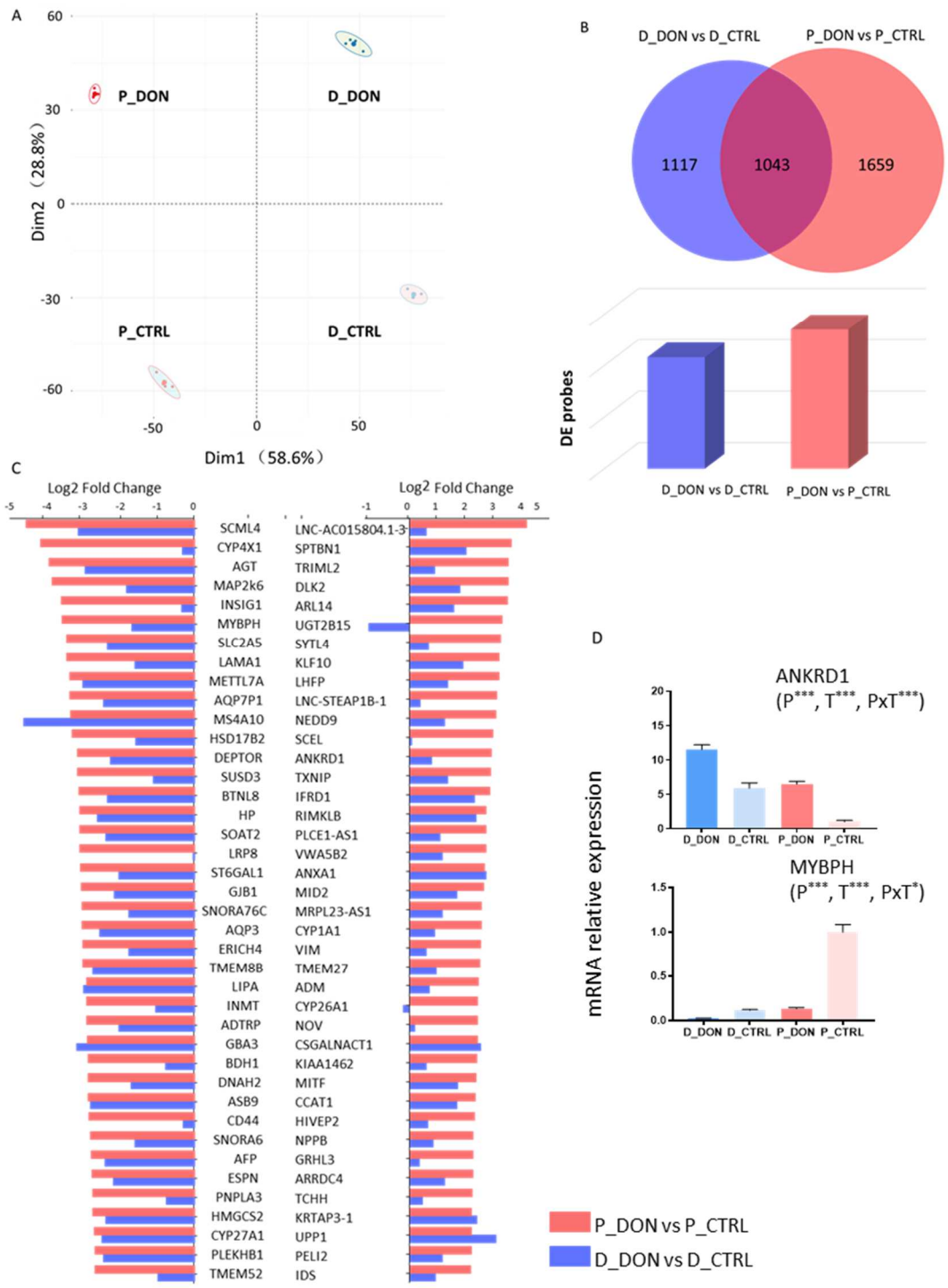

Figure 3. Comparative effect of DON on the genes expression of proliferative and differentiated intestinal epithelial cells.

Proliferative and differentiated cells were exposed to 3 µM DON for 24h. (A) Principal component analysis of samples relationship. (B) Venn diagram comparing differentially expressed genes (FDR p-value ≤ 0.05, FC ≥ 2) in response to DON

exposure in proliferative and differentiated Caco-2 cells. Number of DE genes in the differentiated and proliferative cells upon DON exposure (bottom panel). (C) Top 40 significantly down-regulated and up-regulated genes in proliferative (red bars) and differentiated (blue bars) cells. The values expressed as fold change (in log2) relatively to control cells. (D) Relative mRNA expression by qPCR of two representative genes: ANKRD1 (up-regulated gene) and MYBPH (down-regulated gene). Data were analyzed by non-parametric t-test; T: treatment effect; P: phenotype effect, TxP: interaction *$p < 0.05$; **$p < 0.01$; ***$p < 0.001$.

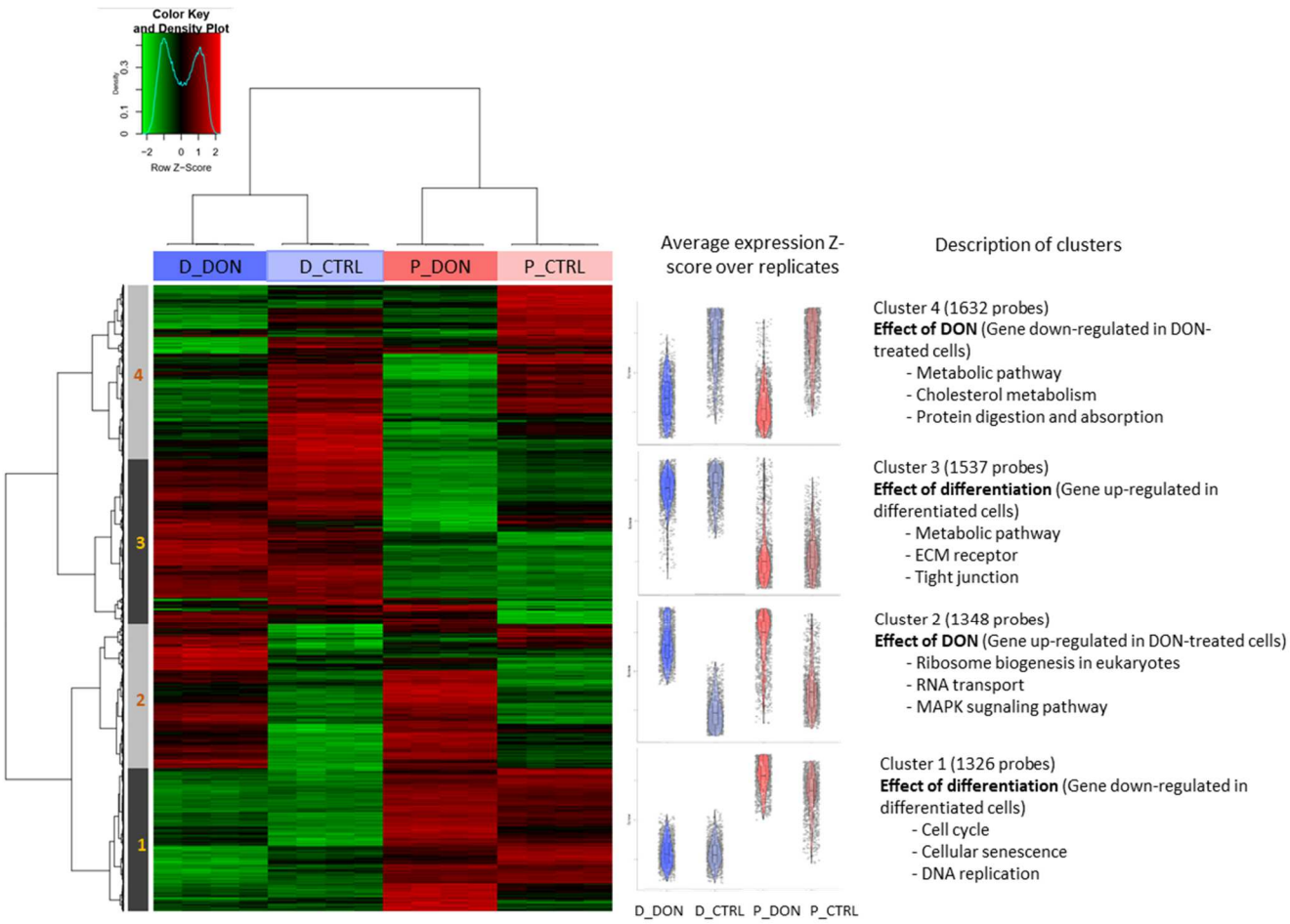

Figure 4. Heat-map depicting the differentially expressed genes between proliferative and differentiated Caco-2 cells exposed to DON.

Proliferative and differentiated cells were exposed to 3 µM DON for 24h. (A) Gene expression was analyzed with a 60K microarray. Red and green indicate values above and below the mean averaged centered and scaled expression values (Z score), respectively. Black indicates values close to the mean. The probe clustering (left panel), delineated 4 gene clusters that are described on the right of the heatmap.

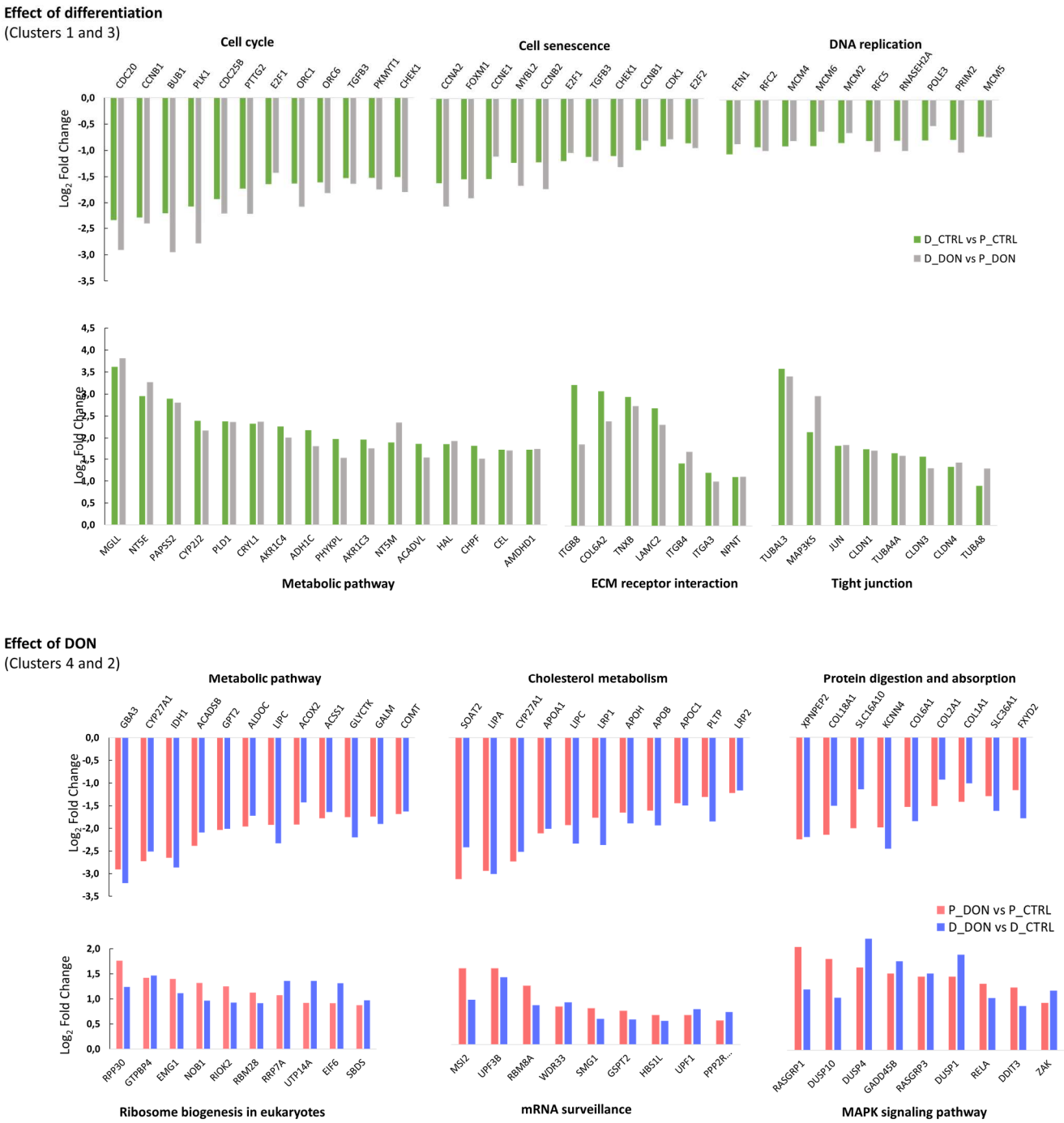

Figure 5. Gene expression analysis of the different clusters.

Proliferative and differentiated cells were exposed to 3 µM DON for 24h and gene expression was analyzed by microarray. 4 clusters depicting the effect of the cell status (cluster 1 and 3) and the effect of the DON treatment (cluster 2 and 4) were identified by a supervised hierarchical clustering analysis. Enriched KEEG pathways ($p \leq 0.05$) was used to analyze in each cluster the relative mRNA expression of differentiated genes each cluster are presented.

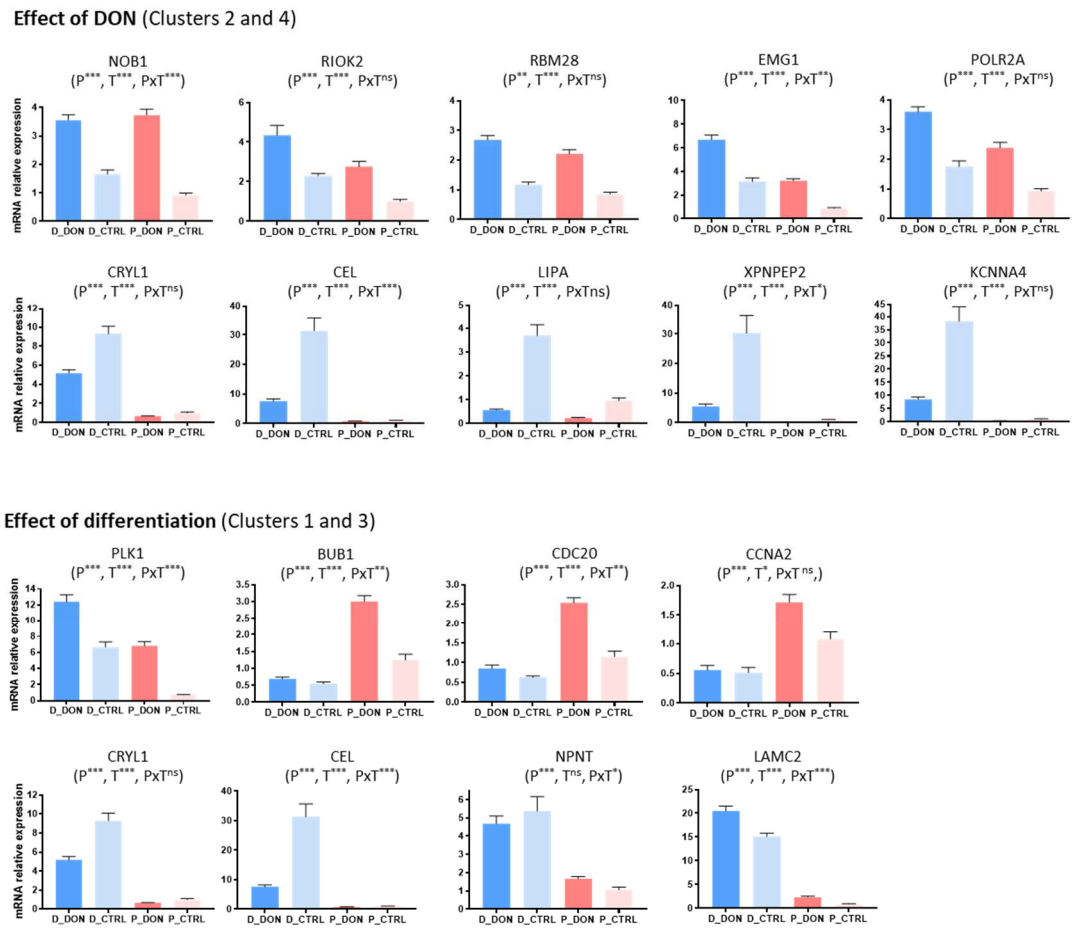

Figure 6. qPCR analysis of representative genes from each cluster.

Proliferative and differentiated cells were exposed to 3 µM DON for 24h and gene expression was analyzed by qPCR. Results are expressed as the mean of 4 independent experiments ± SEM. Data were analyzed by two-way ANOVA after log transformation, T: treatment effect; P: phenotype effect, TxP: interaction *$p < 0.05$; **$p < 0.01$; ***$p < 0.001$.

Gene symbol	Gene name	Primer sequence	Reference
TREML2	Triggering Receptor Expressed on Myeloid cells Like 2	F: CATCTGGACAACATCCTCAA	ENST00000483722.2
		R: CCATCACACCAGTGGTAAA	
ANKRD1	Ankyrin D1	F: CAATCCAGATGTTTGTGATGAG	ENST00000371697.3
		R: GCTCCAGCTTCCATTAACT	
PLK1	polo-like kinase 1	F: CAATCCAGATGTTTGTGATGAG	ENST00000300093.9
		R: GCTCCAGCTTCCATTAACT	
BUB1	Mitotic Checkpoint Serine/Threonine Kinase	F: CCACAATGACCCAAGATTCA	ENST00000302759.11
		R: GGATGACAGGGTTCCAATC	
MYBPH	Myosin Binding Protein H	F: CATCGGCAACTCGTACTC	ENST00000255416.9
		R: CTGAGAAGTCTCGCTCAATAA	
CDC20	Cell Division Cycle 20	F: AAGACCTGCCGTTACATTC	ENST00000372462.1
		R: ACATTCCCAGAACTCCAATC	
CCNA2	Cyclin A2	F: ACTGCTGCTATGCTGTTAG	ENST00000618014.1
		R: ACTTGTTTCTTGGTGTAGGT	
LAMC2	laminin gamma2	F: GGCTCACCAAGACTTACAC	ENST00000264144.5
		R: CGCAGTAACCTTCGATACTC	
NPNT	Nephronectin	F: CGATGCAAACATGGTGAATG	ENST00000379987.6
		R: GCATAACCAGGATGACACTT	
CRYL	Crystallin Lambda 1	F: ACATTGAGCAACAGCAGATA	ENST00000298248.12
		R: AGGGAGCCTTTCAGAGAA	
CEL	Carboxyl Ester Lipase	F: AGACTGCCTGTACCTCAA	ENST00000673714.1
		R: CCTCCATAGATCCAGATCATAAC	
EMG1	Ribosomal RNA Small Subunit Methyltransferase NEP1	F: ACACAAGCTCAGTGTTCG	ENST00000599672.6
		R: TGCCAACTTTCATACATCCA	
NOB1	NIN1 (RPN12) Binding Protein 1 Homolog	F: GGTTCAAGGAGCCCTTAC	ENST00000268802.10
		R: CAACAAACTCTGCTTCCAAC	
RIOK2	RIO Kinase 2	F: TCACAGACTAGGAAGAACCT	ENST00000283109.8
		R: TGGCAGAGAGACGAGATAA	
RBM28	RNA Binding Motif Protein 28	F: CAGAAGAGAGCAGTCAAGAG	ENST00000223073.6
		R: AGTTCCTCTCCATCATCAATAC	
POLR2A	RNA Polymerase II Subunit A	F: GAGGACTCTCAGGAGAAGAA	ENST00000572844.1
		R: CCATGCCCAGCACAAA	
LIPA	lipase A	F: CTGTGTGGATTTAATGAGAGAAA	ENST00000456827.5
		R: CTGGCTCCAGTGTAACAT	
XPNPEP2	X-Prolyl Aminopeptidase 2	F: AGGGCAGGATGTGAGAAA	ENST00000371106.4
		R: GGATGATGTAGGCTGAGAGA	
KCNN4	Potassium Calcium-Activated Channel subfamily N member 4	F: GAGAGGCAGGCTGTTAATG	ENST00000648319.1
		R: GATGGTCAGGAATGTGATGG	
GAPDH	Glyceraldehyde-3-Phosphate dehydrogenase	F: TCAAGGCTGAGAACGGGAAG	ENST00000229239.1
		R: CCACTTGATTTTGGAGGGATCTC	
PSMB6	Proteasome Subunit Beta-Type 6	F: CAGAACAACCACTGGGTCCTACA	ENST00000270586.8
		R: AGCAGAAAATGCGGTCGTG	
ACTIN	Actin Beta	F: AGGCCCCCCTGAACCC	ENST00000432588.17
		R: ATCACGATGCCAGTGGTACG	

1

2 Table 1. Nucleotide sequences of primers for real-time qPCR

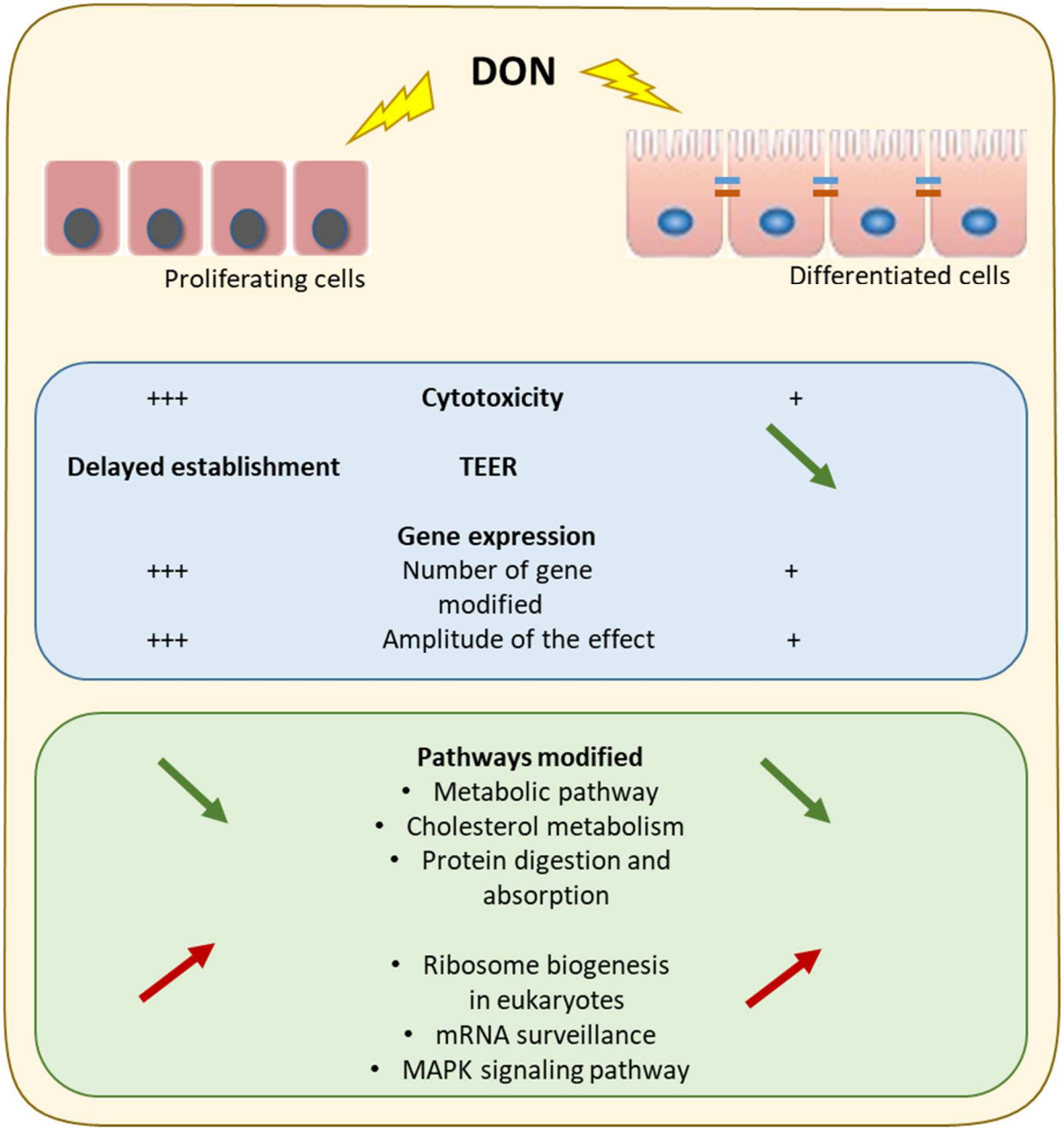
DON
Proliferating cells
Differentiated cells
+++
Cytotoxicity
+
Delayed establishment
TEER
Gene expression
+++
Number of gene modified
+
+++
Amplitude of the effect
+
Pathways modified
• Metabolic pathway
• Cholesterol metabolism
• Protein digestion and absorption
• Ribosome biogenesis in eukaryotes
• mRNA surveillance
• MAPK signaling pathway